Comparison of the peroxidase activities of iron oxide nanozyme with DNAzyme and horseradish peroxidase

Chang Lu[1, 2], Mohamad Zandieh[2], Jinkai Zheng[1*] and Juewen Liu[2*]

1. Institute of Food Science and Technology, Chinese Academy of Agricultural Sciences, Beijing 100193, P. R. China

Email: zhengjinkai@caas.cn

2. Department of Chemistry, Waterloo Institute for Nanotechnology, University of Waterloo, Waterloo, Ontario, Canada

Email: liujw@uwaterloo.ca

Abstract

Peroxidase-based assays are the most extensively used in bioanalytical sensors because of their simple colorimetric readout and high sensitivity owing to enzymatic signal amplification. To improve the stability, modification, and cost of protein-based enzymes, such as horseradish peroxidase (HRP), various enzyme mimics, such as DNAzymes and nanozymes, have emerged over the last few decades. In this study, we compared the peroxidase activities of HRP, a G-quadruplex (G4)-hemin DNAzyme, and Fe_3O_4 nanozymes in terms of activity and stability under different conditions. The reactions were much slower at pH 7 than at pH 4. At pH 4, the turnover rate of HRP (375 s^{-1}) was faster than that of G4 DNAzyme (0.14 s^{-1}) and Fe_3O_4 (6.1×10^{-4} s^{-1}, calculated by surface Fe concentration). When normalized to mass concentrations, the trend was the same. Through observation of the reaction for a long time of 2 h, the changes in the color and UV-vis spectra were also different for these catalysts, indicating different reaction mechanisms among these catalysts. Moreover, different buffers and nanozyme sizes were found to influence the activity of the catalysts. Fe_3O_4 showed the highest stability compared to HRP and G4 DNAzyme after a catalytic reaction or incubation with H_2O_2 for a few hours. This study helps understand the properties of catalysts and the development of novel catalysts with enzyme-mimicking activities for application in various fields.

Keywords

Peroxidase, catalysis, nanozymes, DNAzymes, Fe_3O_4

Introduction

Peroxidase-based assays, such as using horseradish peroxidase (HRP)-labeled antibodies for immunohistochemistry,[1,2] and enzyme-linked immunosorbent assays (ELISA)[3,4] are very popular because of their high sensitivity. However, HRP is a relatively expensive protein that undergoes irreversible denaturation. In addition, it is difficult to perform site-specific labeling on HRP.[5] To solve this problem, many enzyme mimics have been developed.[6-10]

For example, HRP-mimicking DNAzymes (hemin-incorporated G-quadruplex DNA strands) were reported.[11,12] G-quadruplexes (G4s) are non-canonical nucleic acid structures with stacked G-tetrads assembled by Hoogsteen hydrogen bonding. They can bind hemin to form a G4/hemin DNAzyme complex with HRP-mimicking activity. G4/hemin is capable of catalyzing the peroxidation of a diverse range of substrates,[13] resulting in colorimetric, fluorescent, electrochemical, chemiluminescent, electrochemiluminescent, and photoelectrochemical signals for widespread analytical applications.[14-17] Compared to HRP, it is easier to modify DNAzymes, although this type of DNAzymes have lower activities.[18]

In 2007, the peroxidase-like activity of Fe_3O_4 nanoparticles was reported.[19] Although many other nanomaterials also showed similar HRP-like activities, Fe_3O_4 has by far been the most studied due to its cost-effectiveness, high stability and magnetic properties.[20,21] Nanozyme-based biosensors are expected to be more cost-effective and have better stability while keeping the advantages of natural enzymes such as catalytic turnover.[22-24]

Many comparisons have been made for DNAzymes and HRP,[25-28] and also for HRP and Fe_3O_4 nanozymes.[29-34] However, little is known about the side-by-side comparison of these three types of catalysts. In this study, we compared the peroxidase activities of HPR, a DNAzyme and nanozymes in terms of activity and stability under different conditions.

Materials and Methods

Chemicals

The G-rich (PS2.M DNA is 5′-GTGGGTAGGGCGGGTTGG-3') was purchased from Integrated DNA Technologies (Coralville, IA, USA). All metal salts and buffers were purchased from Sigma-Aldrich and Mandel Scientific (Guelph, Ontario, Canada), respectively. Iron Oxide (large Fe_3O_4), hemin, Horseradish peroxidase (HRP), and 1, 3, 5-trimethylbenzene (TMB) were from Sigma-Aldrich. Small Fe_3O_4 NPs were synthesized according to our previous method.[35] The

other chemicals utilized here were of analytical grade. Hemin was dissolved in dimethyl sulfoxide (DMSO) to prepare a stock solution. Milli-Q water was used to prepare all the buffers and solutions.

Peroxidation of TMB

Stock solutions of TMB (81.6 mM) were prepared with DMSO as the solvent. For DNAzyme-catalyzed oxidation, 500 nM PS2.M DNA was annealed in 4 mM $MgCl_2$, 20 mM KCl, and 0.10 M buffer (pH 4 NaAc−HAc or pH 7 phosphate buffer, PB) at 85°C for 10 min. Hemin (500 nM) was then added to the solution. After incubation at 25°C for 30 min, 8.8 mM H_2O_2 and 0.816 mM TMB were added for the oxidation reaction, and the kinetics of absorbance at 652 nm were measured using a microplate reader (Tecan Spark). For HRP or nanozyme-catalyzed oxidation, TMB, H_2O_2, and HRP (or Fe_3O_4) were mixed with 0.10 M buffer (pH 4 acetate or pH 7 PB) with final concentrations of 0.816 mM, 8.8 mM, and 0.02 mg/L for HRP (or 110 mg/L for Fe_3O_4), respectively. Product formation was monitored by measuring the absorbance of $TMB^{\cdot+}$ at 652 nm, which has an extinction coefficient of 39 000 M^{-1} cm^{-1}. The catalytic turnover rates were calculated based on the molar concentration of each catalyst, where the molar concentration of the oxidized TMB product was obtained from the plot of absorbance versus reaction.

Evaluation of the Stability of the Catalysts

DNAzyme, HRP, and Fe_3O_4 were used to catalyze the peroxidation reactions according to the above steps, and then the same concentrations of TMB/H_2O_2 or different enzymes were added to the solutions to continue the reaction, followed by UV-vis absorbance measurements. To evaluate the stability of the catalysts under H_2O_2 treatment, 8.8 mM H_2O_2 was incubated overnight with DNAzyme, HRP, or Fe_3O_4 at 25 °C in the dark. The oxidation reaction was conducted for 120 min, after which 8.8 mM H_2O_2 was added to the solution for further reactions.

Results and Discussion

The Three Catalysts

We purchased an HRP sample (schematically shown in Figure 1A) with a labeled activity of ≥ 250 unit/mg. The DNAzyme named PS2.M with a hemin is shown in Figure 1B. Fe_3O_4 NPs of two sizes were used: 10 nm and 50 nm (Figure 1C and 1D for TEM). It was recently reported that larger Fe_3O_4 NPs have higher peroxidase-like activity.[32] We used TMB as a model substrate to compare their activities, the two-step oxidation reaction of which is well understood (Figure

1E). The first step produces a one-electron oxidation charge-transfer dimer formed between an unreacted substrate and a radical cation. This product exhibited two absorption peaks at 369 nm and 652 nm, respectively, and the latter peak is responsible for the blue color. Further oxidation produces a new two-electron diimine oxidation product with an absorption peak at 450 nm (TMB^{2+} with the yellow color).[36] This yellow product is stable at low pH. The unreacted TMB substrate exhibits an absorption peak at 288 nm and is thus colorless.

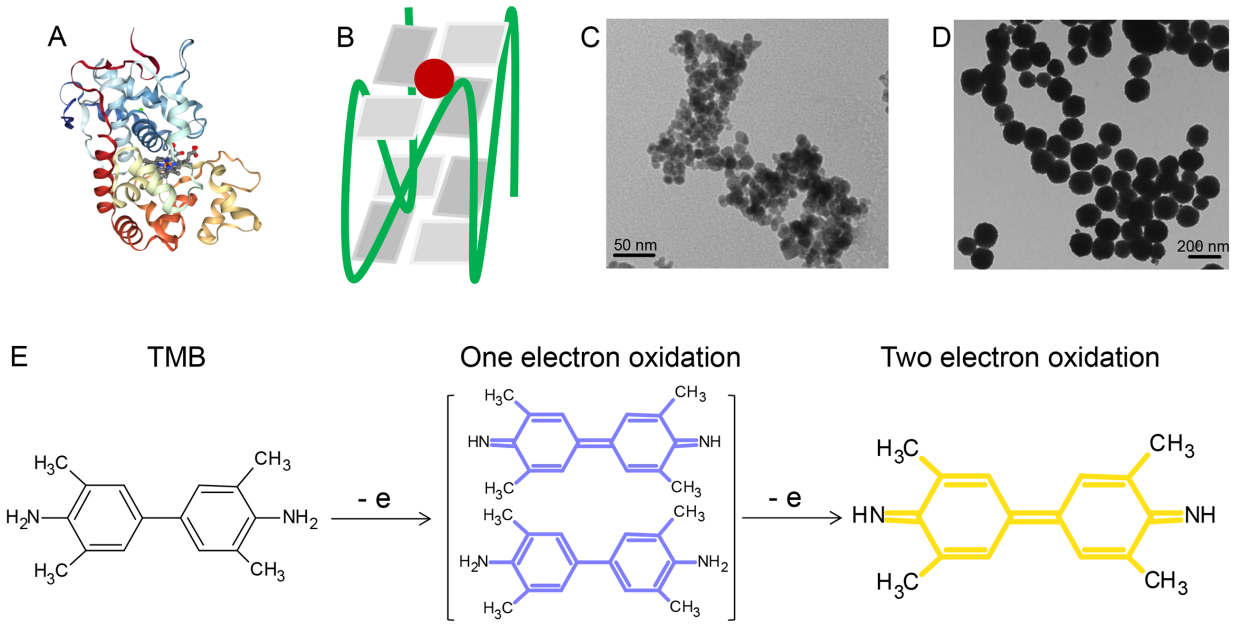


Figure 1. Cartoon representation of (A) a HRP and (B) a PS2.M DNAzyme with a hemin cofactor. TEM micrographs of (C) small 10 nm and (D) large 50 nm Fe_3O_4 NPs used in this study. (E) Scheme of two-step TMB oxidation reaction.

Activity Comparison at pH 4

The activity of the peroxidation catalyst is strongly affected by pH, and pH 4 is the optimal pH for most nanozymes using TMB as a substrate.[37,38] Therefore, we first tested their activities at pH 4.0. To investigate the peroxidase activity, the time-dependent change in the absorption at 652 nm for the blue TMB oxidation product was monitored. Since the activity of HRP was very high, we only used 0.5 nM HRP, which was 1000-fold lower than that of the DNAzyme (0.5 μM or 3.18 mg/L). We then calculated and compared the turnover rate of the catalysts, which is defined as the moles of substrate converted into product by one mole of enzyme per unit time. Since the

absorbance value of the DNAzyme sample decreased after 50 min, our calculation only covered the initial rising stage (ESI, Calculations #1). Based on the concentration of the oxidized TMB product, the turnover rate of HRP reaction was 375 s^{-1}, whereas the turnover rate of the DNAzyme was 0.140 s^{-1} (Figure 2A). Therefore, at the same molar concentration, HRP was ~2700-fold more active than the DNAzyme. Since the molecular weight of HRP is 40,000 Da, and the molecular weight of the DNAzyme is 5,708 Da, at the same mass concentration, the difference decreased to approximately 430-fold (ESI, Calculations #2).

For 50 nm Fe_3O_4, we used a concentration of 110 mg/L for the initial experiment, which corresponded to the same molar concentration as HRP (0.5 nM), assuming homogeneous spheres (ESI, Calculations #3). Considering molar concentration of Fe_3O_4 (each NP = 1 nanozyme unit), the turnover rate was calculated to be 34.2 s^{-1} suggesting an only 10-times lower activity than HRP and ~250-fold higher activity than the DNAzyme. Because each Fe_3O_4 NP consists of many catalytically active Fe atoms, this calculate could overestimate the activity of individual Fe_3O_4 active sites. We then calculated the molar concentration of surface iron atoms to be 28 μM (ESI, Calculations #3). Therefore, the turnover rate of Fe_3O_4 was calculated to be 6.10×10^{-4} s^{-1} based on the surface Fe atoms, indicating a 230-fold lower activity than the DNAzyme.[39] We previously calculated the turnover rate of 300 nm Fe_3O_4 NPs for TMB peroxidation to be 9.2×10^{-3} s^{-1}. Considering the smaller size of the NPs used in this work, the turnover rate was reasonably lower than the 300 nm NPs.[24,32] Similarly, when normalized to the same mass concentration, the DNAzyme was ~145-fold faster than Fe_3O_4 (Figure 2A). A comparison of the turnover rates of these catalysts, based on different normalizations, is summarized in Table 1.

After the reaction, the color of the products also differed for different catalysts. The DNAzyme sample turned yellow and its UV-vis spectrum showed an intense peak at 450 nm (almost no peak at 652 nm, Figure 2B), indicating that the blue product was converted to the two-electron oxidation product. However, this did not occur for HRP, whose product was mostly blue (intense peak at 652 nm and a very small peak at 450 nm). With the very high activity of HRP, its product remained blue, suggesting that peroxidation by the DNAzyme was stronger and less controlled. This may suggest a different reaction mechanism between the two enzymes, despite both use hemin as a cofactor.

The DNAzyme system has a more loosely bound hemin, and a fraction of free hemin might be present, which may oxidize the substrate non-specifically.[40] We then performed a

control experiment with only free hemin (no DNA), and the color of the product was also yellow (Figure 2E, F). Compared to the samples with DNAzyme, less blue one-electron oxidation product was observed, and the blue peak started to decrease after approximately 35 min. With DNAzyme (at 1:1 with hemin), the blue product peaked at approximately 50 min, and the peak intensity was ~2.5-fold that of the free hemin sample. If the concentration of DNAzyme exceeded 5-fold of hemin, the blue peak appeared at approximately 60 min and reached an even higher absorbance value before it started to drop (Figure 2E). Therefore, we reason that oxidation by free hemin was the main reason for the further oxidation of the system to the yellow product.

The oxidation product of Fe_3O_4 was blue even after approximately 2 h (Figure 2A), indicating that the reaction stopped at the one-electron oxidation stage. Most previous studies monitored the reaction only for a short time, and thus even the DNAzyme product showed mostly blue color. By monitoring the reaction for a longer period of time, we obtained new insights.

Activity Comparison at pH 7

We then repeated the experiments at pH 7, where the reactions were much slower overall. An HRP concentration of 5 nM (10-fold higher than that at pH 4) was used to achieve a similar initial reaction kinetic slope (Figure 2C). After 15 min, the peak at 652 nm started to decay. However, no sign of yellow coloration was observed. Most of the absorbance was below 300 nm, which corresponds to the TMB substrate. Therefore, the product appeared to convert back to its substrate state, as indicated by the strong absorbance below 300 nm.

We used 500 nM DNAzyme at pH 7, which was 100-fold higher than that of HRP. The activity of DNAzyme was still lower. For G4 DNAzyme, we also observed the disappearance of blue color without the appearance of yellow color. Therefore, the blue product is unstable at pH 7. Finally, we observed no oxidation products with the Fe_3O_4 NPs. Among them, still HRP showed the highest activity at pH 7. Therefore, at both low and neutral pH, HRP showed the best activity, while the nanozyme had the lowest activity.

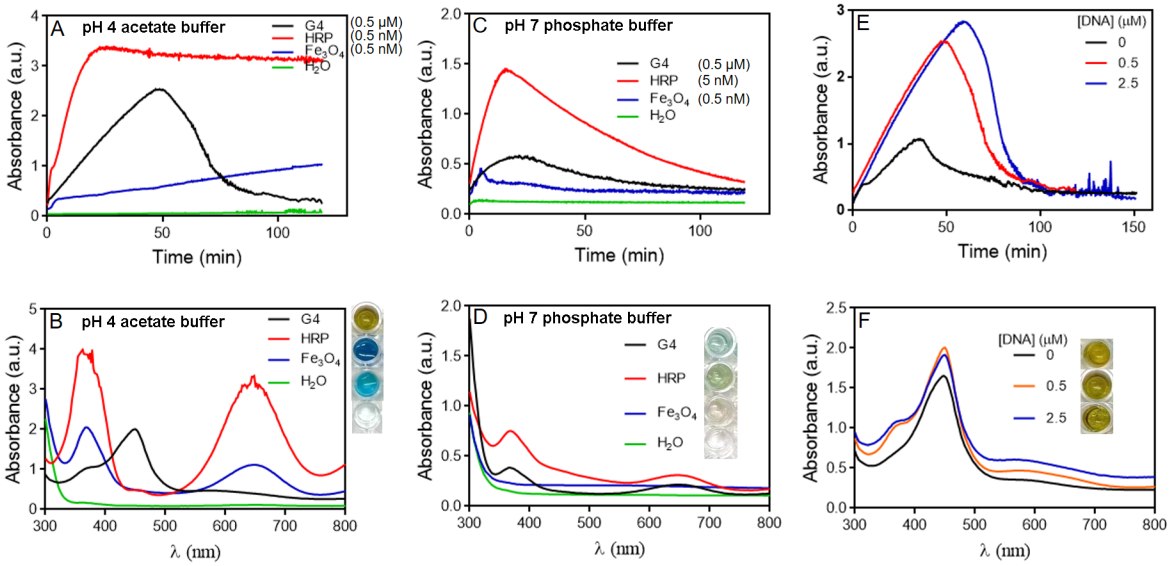


Figure 2. Activity and kinetics comparison monitored at 652 nm for different catalysts in (A, B) pH 4.0 acetate buffer and (C, D) pH 7.0 PB. (E, F) Activity of G4 DNAzyme at different DNA concentrations. (A, C, E) The kinetic traces; (B, D, F) the UV-vis spectra of the final reaction products.

Table 1. Comparison of catalytic activities using different enzyme units. The slope of kinetic traces are calculated from data in the first 20 min.

	DNAzyme	HRP	Fe_3O_4 (50 nm)
Mass concentration (mg/L)	3.18	0.02	110
Molar concentration (μM)	0.50	0.50×10^{-3}	0.50×10^{-3} (NPs concentration)
			28.0 (surface Fe atom concentration)
Turnover rate (s^{-1})	0.14	375	34.2 (each NP = 1 active site)
			6.1×10^{-4} (each surface Fe = 1 active site)
Rate normalized to mass concentration (s^{-1}/mg. L^{-1})	2.9×10^{-4}	0.125	2.0×10^{-6}

Effect of buffer

Since pH 4 has optimal activities, we focused our study on pH 4. We then tested the activities of the three catalysts in different buffers, which can also affect enzyme activity.[41] At pH 4, citrate, acetate and phosphate (PB) buffers were tested (Figure 3A). In the three pH 4 buffers, the activity of HRP was initially similar (in the first 5 min). After 5 min, the activity in citrate buffer decreased significantly. After 120 min, we measured the UV-vis spectra (Figure 3D). In acetate buffer, the one-electron oxidation blue product was dominant. In contrast, almost no products were observed in the citrate buffer. Since citrate is a reducing agent, we reasoned that the decay of the blue-colored product was due to its reduction by citrate.

For the DNAzyme, in the first 10 min, a similar one-electron oxidation blue product was observed in all buffers, but the color in the citrate buffer also decayed (Figure 3B). In addition, the blue product in the acetate buffer also decreased. In the case of the DNAzyme, the blue color was converted to yellow products, and the generation of yellow products in the acetate buffer was much faster. After 2 h, the product remained blue in PB (Figure 3E). This suggested that the activity of the DNAzyme was higher in the acetate buffer than in the PB buffer, and it can be explained by that acetate can also mediate peroxidation reactions.[42]

For Fe_3O_4 NPs (50 nm), the reaction was observed only in the acetate buffer, and no yellow product was observed after 2 h (Figure 3C, F). These results indicated that the oxidizing capacities of the catalysts at pH 4 differed in different buffers. Acetate allowed the highest activity, PB can be used for HRP and the DNAzyme, but citrate can hinder the oxidizing capacity of the enzymes for TMB.[43]

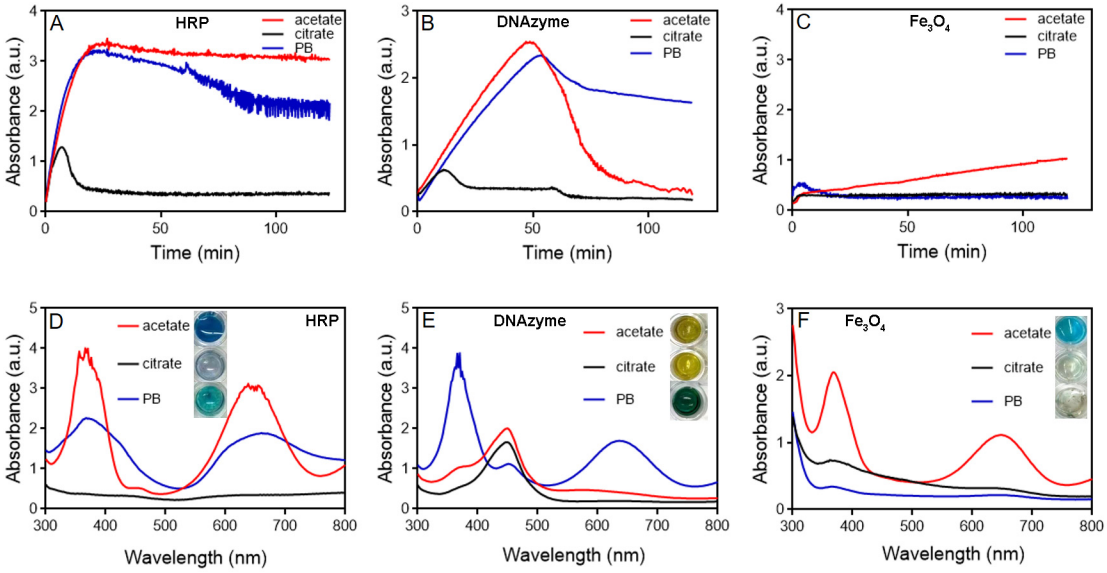


Figure 3. The reaction kinetics and final UV-vis spectra of (A and D) HRP, (B and E) G4 and (C and F) Fe_3O_4 catalyzed reactions in different pH 4 buffers (acetate, citrate, and PB).

Small and large Fe_3O_4 NPs

The activity of Fe_3O_4 NPs of different sizes was also compared in acetate buffer (pH 4). The 10 nm and 50 nm Fe_3O_4 NPs with the same mass concentration showed very similar activities, and both samples turned blue, indicating the one-electron oxidation (Figure 4A, B). While there are more surface metal atoms for the smaller Fe_3O_4 NPs, if normalized to the same iron atom concentration, the activity for the large Fe_3O_4 was higher. From our quantitative calculations, the turnover rate of the 10 nm Fe_3O_4 NPs was 0.24 s^{-1} (each NP = 1 active site) or 1.1×10^{-4} s^{-1} (each surface Fe = 1 active site), which were both slower than that of the large Fe_3O_4 NPs (ESI, Calculations #1 and 3). This was explained by higher polycrystallinity of larger Fe_3O_4 NPs, resulting in a higher Fe^{2+}/Fe^{3+} ratio.[32] DLS showed the size of the Fe_3O_4 NPs were about 1-2 μm (Figure 4C), much larger than the original Fe_3O_4 NPs (10 to 50 nm), which may result from the aggregation of the Fe_3O_4 NPs.

As shown in Figure 4D, in pH 4 acetate buffer, both Fe_3O_4 NPs had similar positive zeta potentials (approximately 20 mV). In pH 7 PB buffer, these two Fe_3O_4 NPs showed a negative zeta potential (about -20 mV). However, in pH 7 MOPS buffer, the large Fe_3O_4 NPs were close charge neutral, which can compromise the colloidal stability. The more negative zeta-potential in PB suggests the adsorption of phosphate to Fe_3O_4 NPs.[44] Such adsorption can also change

nanozyme activities because of the surface modification to affect substrate/product adsorption.[45-47] In turn, this can result in different oxidizing activities of Fe_3O_4 NPs in different buffers.

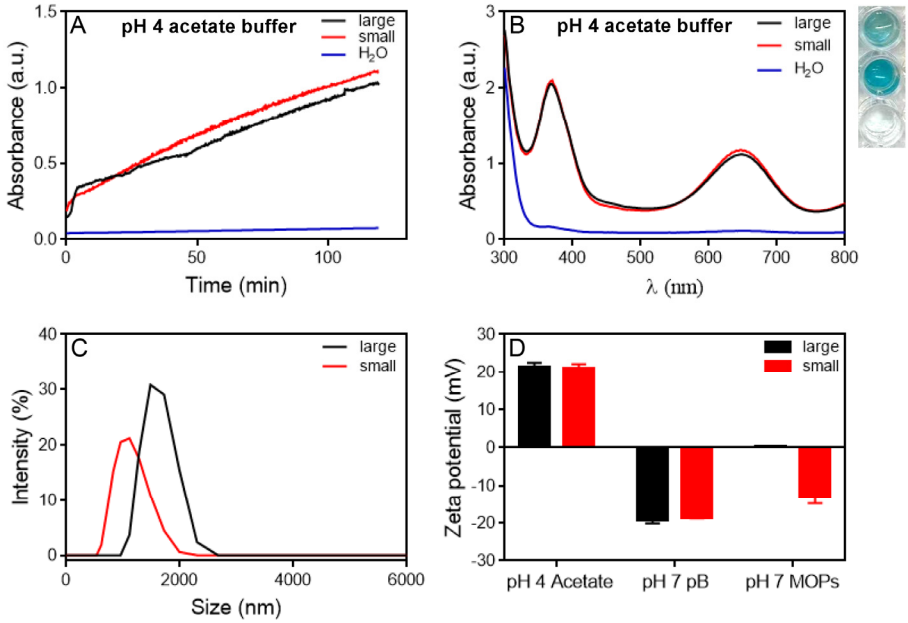


Figure 4. (A) Reaction kinetics and (B) final product UV-vis spectra of TMB peroxidation with small 10 nm and large 50 nm Fe_3O_4 NPs in pH 4 acetate buffer. (C) DLS and (D) zeta potentials of the small and large Fe_3O_4 NPs.

Stability of the Catalysts

The promise of nanozymes and DNAzymes is that they may be more stable than protein enzymes. To investigate their stability, the three different catalysts were first used to catalyze the oxidation of TMB in the presence of H_2O_2 in pH 4 acetate buffer. As shown in Figure 5, after 120 min, the reactions reached saturation for HRP and the G4 DNAzyme, although the Fe_3O_4 reaction continued. Then, additional TMB and H_2O_2 or additional enzymes were added at the 120 min time point.

For HRP, little absorbance change was observed after adding additional HRP or extra HRP with H_2O_2 (Figure 5A and 5D; Figure S1), suggesting that the system saturation might be due to running out of the substrate. However, when additional TMB and H_2O_2 were added, still no further color increase was observed, suggesting that HRP lost its activity after the catalytic reaction.

For the DNAzyme, adding TMB immediately increased the blue product (Figure 5B and 5E). The color remained stable and did not change to yellow after further incubation. This was attributed to the formation of a charge-transfer complex consisting of diamine (TMB) as the donor and diimine dication (TMB^{2+}) as the acceptor. Therefore, in the G4 system, catalytic activity disappeared after the reaction. It appears that hemin was degraded. Otherwise, free hemin could further convert the blue product to yellow. Degradation of hemin in such DNAzymes was recently reported by the Fu group.[28]

For Fe_3O_4, more blue product was observed when additional TMB and H_2O_2 were added (Figure 5C and 5F), confirming its higher stability. When additional Fe_3O_4 was added, a jump was also observed, but the peak gradually decreased, which was attributed to further oxidation of TMB to a yellow product, since the sample appeared yellowish and a small peak at 450 nm emerged.

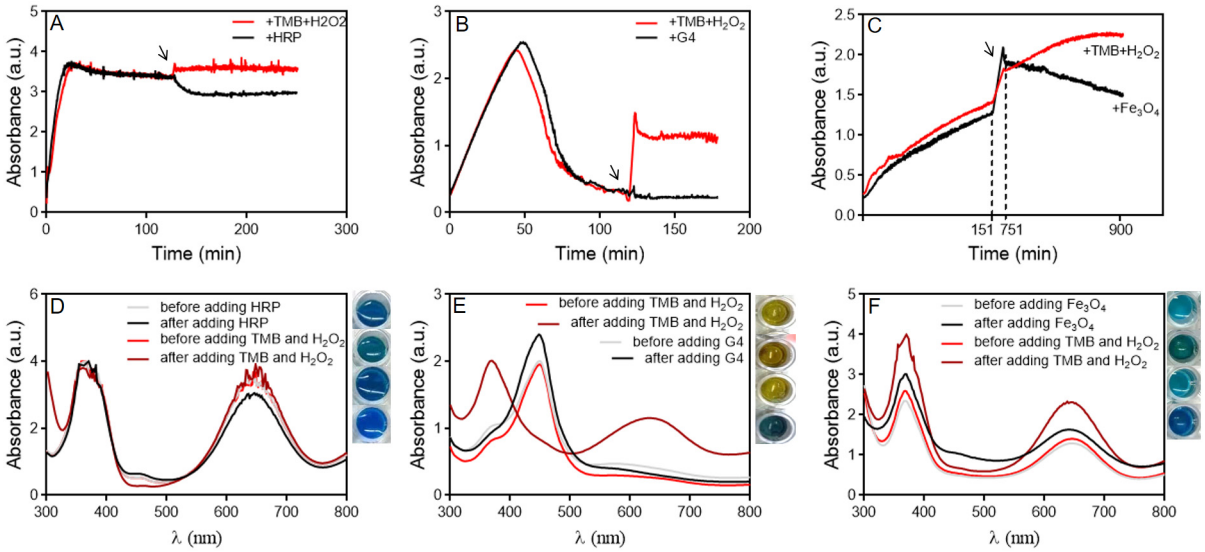


Figure 5. Evaluation of the stability of (A and D) HRP, (B and E) G4 DNAzyme, and (C and F) Fe_3O_4 after catalysis of TMB oxidation in a pH 4 acetate buffer based on the reaction kinetics monitored at 652 nm and final product spectra. At 120 min, additional reagents were added.

Then, stability was tested by incubating different enzymes with H_2O_2 overnight, adding TMB for the oxidation reaction, and then adding more H_2O_2. As shown in Figure 6, no reaction was observed with HRP, indicating that HRP was inactivated after long-term incubation with H_2O_2.[48] While for the G4 DNAzyme, the reaction became slower compared with the control group and blue product was observed after the reaction (Figure 6B, E). After adding H_2O_2, the

activity increased and became similar to the initial activity of the control sample, which may be attributed to the decrease in H_2O_2 after incubation with G4 DNAzyme. For Fe_3O_4, the activity was stable after overnight incubation (Figure 6C and F). This indicates that Fe_3O_4 is a poor catalase mimic and that H_2O_2 can be quite stable in the presence of Fe_3O_4. Based on our data in this work, we summarized the comparisons in Figure 7.

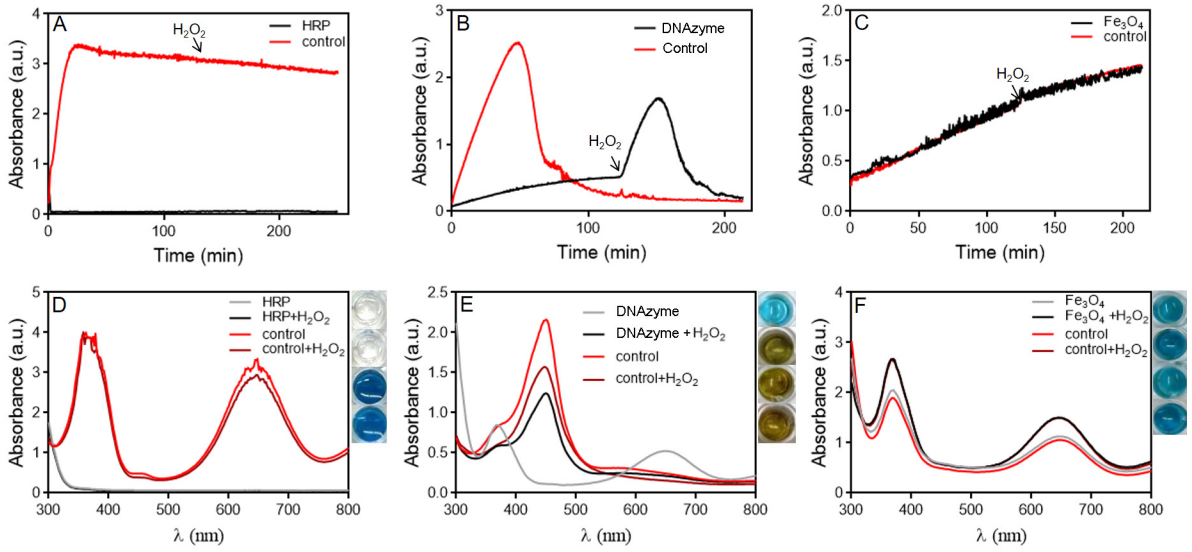


Figure 6. Stability study of (A and D) HRP, (B and E) G4 DNAzyme, and (C and F) Fe_3O_4 before and after overnight incubation with H_2O_2. The absorbance at 652 nm was monitored for the kinetic studies. Control samples mean normal reaction conditions without overnight pre-incubation with H_2O_2. At the time point of 120 min indicated by the arrowheads, additional 8.8 mM H_2O_2 was added. Control means normal reaction conditions, while the other lines in (A-C) are for the overnight incubated samples.

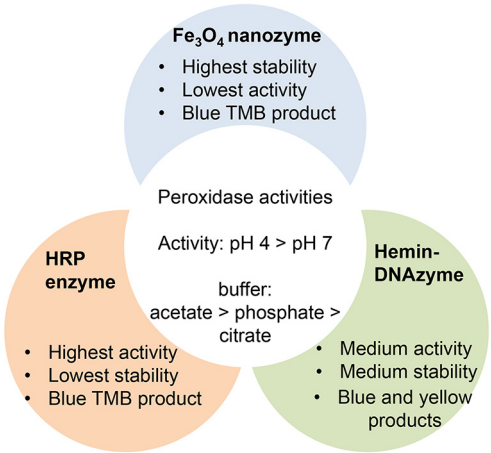


Figure 7. A summary showing the similarities and differences between these three catalysts.

Conclusions

In summary, the peroxidase activities of enzymes, DNAzymes and nanozymes were compared in this work, from the aspects of both activities and stabilities in different conditions**.** Overall, the reactions were much slower at pH 7 than at pH 4.0. At pH 4.0, which is the optimal pH for most peroxidase reactions using TMB, the activity of HRP was faster than that of the G4 DNAzyme and Fe_3O_4 at the same molar or mass concentration. The color of the products was different for these catalysts. After the reaction, the G4 sample had a two-electron oxidation yellow product, while HRP and Fe_3O_4 had a one-electron oxidation blue product, suggesting a different reaction mechanism for the three catalysts. The oxidizing capacity of catalysts differs in different buffers: acetate performs best and PB buffer has little effect on the activities, but citrate can hinder the oxidizing capacity of the catalysts. The stability of the catalysts was also compared. Fe_3O_4 showed high stability, whereas HRP and G4 DNAzyme lost their activities after one catalytic reaction or incubation with H_2O_2 for a few hours. These results may be useful in the future for constructing more efficient catalysts and developing colorimetric assays.

Electronic supplementary information

Stability of HRP after one catalysis of TMB and then adding HRP and H_2O_2 in acetate buffer at pH 4. Calculations: molar concentration and surface Fe atoms of Fe_3O_4 NPs, peroxidase-like catalytic turnover rates of the three catalysts, catalytic activities normalized to mass concentration.

Acknowledgements

Funding for this work was provided by the Natural Sciences and Engineering Research Council of Canada (NSERC), the National Natural Science Foundation of China (31901776 and 32072181), and the Agricultural Science and Technology Innovation Program of the Institute of Food Science and Technology, Chinese Academy of Agricultural Sciences (CAAS-ASTIP-G2022-IFST-06). C. Lu received a China Scholarship Council (CSC) Scholarship to visit the University of Waterloo.

References

1. Y. Zhao, Y. Zheng, R. Kong, L. Xia and F. Qu, *Biosens. Bioelectron.*, 2016, **75**, 383-388.
2. H. Yang, C. S. Bever, H. Zhang, G. M. Mari, H. Li, X. Zhang, L. Guo, Z. Wang, P. Luo and Z. Wang, *Anal. Biochem.*, 2019, **581**, 113336.
3. L. Cohen, N. Cui, Y. Cai, P. M. Garden, X. Li, D. A. Weitz and D. R. Walt, *ACS Nano*, 2020, **14**, 9491-9501.
4. N. Kohmer, C. Rühl, S. Ciesek and H. F. Rabenau, *J. Clin. Med.*, 2021, **10**, 2128.
5. M. Khanmohammadi, M. B. Dastjerdi, A. Ai, A. Ahmadi, A. Godarzi, A. Rahimi and J. Ai, *Biomater. Sci.*, 2018, **6**, 1286-1298.
6. Z. Chen, Z. Wang, J. Ren and X. Qu, *Acc. Chem. Res.*, 2018, **51**, 789-799.
7. X. Zhang, G. Li, G. Chen, D. Wu, Y. Wu and T. D. James, *Adv. Funct. Mater.*, 2021, **31**, 2106139.
8. K. Li, K. Wu, Y. L. Lu, J. Guo, P. Hu and C. Y. Su, *Angew. Chem. Int. Ed.*, 2022, **61**, e202114070.
9. X. Niu, N. Cheng, X. Ruan, D. Du and Y. Lin, *J. Electrochem. Soc.*, 2019, **167**, 037508.
10. R. Tian, Y. Li, J. Xu, C. Hou, Q. Luo and J. Liu, *J. Mater. Chem. B*, 2022, **10**, 6590-6606.
11. F. Li, C. Wang and W. Guo, *Adv. Funct. Mater.*, 2018, **28**, 1705876.
12. X. Gong, X. Li, T. Qing, P. Zhang and B. Feng, *Analyst*, 2019, **144**, 1948-1954.
13. Y. Liu, P. Lai, J. Wang, X. Xing and L. Xu, *Chem. Comm.*, 2020, **56**, 2427-2430.
14. B. Zhai, K. Huang, H. Wang, D. Su and Y. Xu, *Catalysts*, 2021, **11**, 1352.
15. J.-E. Lee, H. Mun, S.-R. Kim, M.-G. Kim, J.-Y. Chang and W.-B. Shim, *Biosens. Bioelectron.*, 2020, **151**, 111968.
16. Z. Salmasi, N. Rouhi, H. Safarpour, N. Zebardast and H. Zare, *Crit. Rev. Anal. Chem.*, 2022, 1-22.
17. S. Khan, B. Burciu, C. D. Filipe, Y. Li, K. Dellinger and T. F. Didar, *ACS Nano*, 2021, **15**, 13943-13969.
18. Z. Su, Q. Wen, S. Li, L. Guo, M. Li, Y. Xiong, W. Li and J. Ren, *Anal. Chim. Acta*, 2022, **1221**, 340143.
19. L. Gao, J. Zhuang, L. Nie, J. Zhang, Y. Zhang, N. Gu, T. Wang, J. Feng, D. Yang, S. Perrett and X. Yan, *Nat. Nanotechnol.*, 2007, **2**, 577-583.
20. H. Dong, W. Du, J. Dong, R. Che, F. Kong, W. Cheng, M. Ma, N. Gu and Y. Zhang, *Nature Commun.*, 2022, **13**, 1-11.
21. J. Ju, Y. Chen, Z. Liu, C. Huang, Y. Li, D. Kong, W. Shen and S. Tang, *Chin. Chem. Lett.*, 2022, 107820.
22. S. Li, X. Zhao, X. Yu, Y. Wan, M. Yin, W. Zhang, B. Cao and H. Wang, *Anal. Chem.*, 2019, **91**, 14737-14742.
23. W. Li, G.-C. Fan, F. Gao, Y. Cui, W. Wang and X. Luo, *Biosens. Bioelectron.*, 2019, **127**, 64-71.
24. M. Zandieh and J. Liu, *ACS Nano*, 2021, **15**, 15645-15655.
25. D. Sun, X. Lin, J. Lu, P. Wei, Z. Luo, X. Lu, Z. Chen and L. Zhang, *Biosens. Bioelectron.*, 2019, **142**, 111578.
26. H. Kamali, S. Golmohammadzadeh, H. Zare, R. Nosrati, M. Fereidouni and H. Safarpour, *J. Nanobiotechnol.*, 2022, **20**, 438.

27. E. Shokri, M. Hosseini, M. N. Boldaji, K. Shahsavar, N. Nasiri, A. Bahmani, M. R. Ganjali and A. A. Saboury, *Mol. Catal.*, 2022, **519**, 112156.
28. A. R. Monte Carlo III and J. Fu, *ChemPlusChem*, 2022, **87**, e202200090.
29. L. Hong-Ying, X. Han-Xiao, Z. Lang-Lang, W. Jia-Jun, Q. Yu-Bin, G. Chun-Chuan and L. Li-Hua, *Chinese J. Anal. Chem.*, 2021, **49**, e21160-e21169.
30. S. R. Ahmed, J. Cirone and A. Chen, *ACS Appl. Nano Mater.*, 2019, **2**, 2076-2085.
31. M. Gumpelmayer, M. Nguyen, G. Molnár, A. Bousseksou, B. Meunier and A. Robert, *Angew. Chem. Int. Ed.*, 2018, **130**, 14974-14979.
32. Y. Qiu, B. Yuan, H. Mi, J.-H. Lee, S.-W. Chou and Y.-K. Peng, *J. Phys. Chem. Lett.*, 2022, **13**, 8872-8878.
33. M. Zandieh and J. Liu, *Adv. Mater.*, 2023, DOI: 10.1002/adma.202211041.
34. B. Jiang, D. Duan, L. Gao, M. Zhou, K. Fan, Y. Tang, J. Xi, Y. Bi, Z. Tong, G. F. Gao, N. Xie, A. Tang, G. Nie, M. Liang and X. Yan, *Nat. Protocols*, 2018, **13**, 1506-1520.
35. M. Zandieh and J. Liu, *Angew. Chem. Int. Ed.*, 2022, **61**, e202212013.
36. X. Zhang, Q. Yang, Y. Lang, X. Jiang and P. Wu, *Anal. Chem.*, 2020, **92**, 12400-12406.
37. L. Gao, K. Fan and X. Yan, *Theranostics*, 2017, **7**, 3207-3227.
38. J. Zhang, S. Wu, X. Lu, P. Wu and J. Liu, *Nano Lett.*, 2019, **19**, 3214-3220.
39. M. Zandieh and J. Liu, *Langmuir*, 2022, **38**, 3617-3622.
40. Z. Wang, J. Zhao, J. Bao and Z. Dai, *ACS Appl. Mater. Interfaces*, 2016, **8**, 827-833.
41. W. Li, Y. Li, Z. Liu, B. Lin, H. Yi, F. Xu, Z. Nie and S. Yao, *Nucleic Acids Res.*, 2016, **44**, 7373-7384.
42. D. Peng, R.-P. Liang, J.-D. Qiu and J. Liu, *J. Anal. Test.*, 2019, **3**, 260-268.
43. W. Lai, J. Guo, Z. Qiao, X. Chen, S. Wang, L. Wu, Q. Cai, S. Ye, Y. Lin and D. Tang, *New J. Chem.*, 2021, **45**, 11977-11982.
44. B. Liu and J. Liu, *Chem. Commun.*, 2014, **50**, 8568-8570.
45. Y. Zhao, H. Li, A. Lopez, H. Su and J. Liu, *ChemBioChem*, 2020, **21**, 2178-2186.
46. Y. Chang, Q. Chen, B. Liu, Z. Zhang, M. Liu and J. Liu, *Inorg. Chem. Commun.*, 2021, **134**, 108979.
47. G. Tang, J. He, J. Liu, X. Yan and K. Fan, *Exploration*, 2021, **1**, 75-89.
48. J. Hernandez-Ruiz, M. B. Arnao, A. N. Hiner, F. Garcia-Canovas and M. Acosta, *Biochem. J.*, 2001, **354**, 107-114.